Immunity
Article

Antigen Availability Determines CD8+ T Cell-Dendritic Cell Interaction Kinetics and Memory Fate Decisions

Sarah E. Henrickson,[1] Mario Perro,[1,4] Scott M. Loughhead,[1,4] Balimkiz Senman,[1,4] Susanne Stutte,[1] Michael Quigley,[2] Gabriela Alexe,[2] Matteo Iannacone,[1] Michael P. Flynn,[1] Shaida Omid,[1] Jonathan L. Jesneck,[2] Sabrina Imam,[2] Thorsten R. Mempel,[3] Irina B. Mazo,[1] W. Nicholas Haining,[2] and Ulrich H. von Andrian[1,*]

[1]Division of Immunology, Department of Microbiology and Immunobiology, Harvard Medical School, Boston, MA 02115, USA
[2]Department of Pediatric Oncology, Dana-Farber Cancer Institute and Children's Hospital Boston, Harvard Medical School, Boston, MA 02115, USA
[3]Center for Immunology and Inflammatory Diseases, Massachusetts General Hospital, Charlestown, MA 02129, USA
[4]These authors contributed equally to this work
*Correspondence: uva@hms.harvard.edu
http://dx.doi.org/10.1016/j.immuni.2013.08.034

SUMMARY

T cells are activated by antigen (Ag)-bearing dendritic cells (DCs) in lymph nodes in three phases. The duration of the initial phase of transient, serial DC-T cell interactions is inversely correlated with Ag dose. The second phase, characterized by stable DC-T cell contacts, is believed to be necessary for full-fledged T cell activation. Here we have shown that this is not the case. CD8+ T cells interacting with DCs presenting low-dose, short-lived Ag did not transition to phase 2, whereas higher Ag dose yielded phase 2 transition. Both antigenic constellations promoted T cell proliferation and effector differentiation but yielded different transcriptome signatures at 12 hr and 24 hr. T cells that experienced phase 2 developed long-lived memory, whereas conditions without stable contacts yielded immunological amnesia. Thus, T cells make fate decisions within hours after Ag exposure, resulting in long-term memory or abortive effector responses, correlating with T cell-DCs interaction kinetics.

INTRODUCTION

When a naive T (Tn) cell exits the thymus, it embarks on a single-minded mission: to find and eliminate pathogens to which it can respond. T cells rely on T cell receptors (TCR), which recognize peptides in major histocompatibility complexes (pMHC) on antigen (Ag)-presenting cells (APCs) (Germain and Stefanová, 1999). In theory, there are billions of Ags for CD8+ T cells, which recognize MHC class I molecules complexed with noncovalently bound peptides. In practice, for a given MHC allele, peptide number is limited by specific residues that determine whether and how long a peptide can be presented (Townsend and Bodmer, 1989). Nonetheless, the diversity of potential T cell Ags is enormous and requires a large repertoire of T cells, each with its own randomly assembled TCR. This need for TCR diversity is balanced by the metabolic cost of T cell generation, so the frequency of Tn cells that express a "cognate" TCR specific for any individual pMHC complex is only 1 in 10^5–10^7 (Blattman et al., 2002; Casrouge et al., 2000).

Ag-specific Tn cells must quickly assess whether an Ag is present, whether it poses a threat, and, if so, what response will be appropriate (Lanzavecchia and Sallusto, 2000). This information is provided to Tn cells by dendritic cells (DCs) in lymph nodes (LNs), which constantly recruit Tn cells from the blood and receive Ag-carrying DCs via afferent lymphatics from nearby tissues (von Andrian and Mempel, 2003). Tn cells migrate rapidly (>10 μm/min) within the LN cortex to query local DCs for the presence of cognate Ag. A single DC can be contacted by ~5,000 T cells/hr (Miller et al., 2004a), and this high scanning efficiency is necessary, in particular for CD8+ Tn cells, because antigenic peptides in MHC class I can dissociate quickly (Zinkernagel and Doherty, 1974). This challenge becomes particularly relevant when Tn cells must respond to transient, nonreplicating Ags, such as recombinant vaccines.

As Tn cells encounter Ag-presenting DCs, they must decide whether or not to respond. For full activation, Tn cells require multiple signals, including TCR recognition of cognate pMHCs, costimulation by B7 family members, and cytokines (Henrickson and von Andrian, 2007). This generates rapidly proliferating effector cells (Teff) that migrate to inflamed tissues where they produce cytokines (especially interferon-γ [IFN-γ]) and kill APCs. Upon Ag clearance, most Teff cells apoptose, but in many settings a few Ag-experienced T cells persist as long-lived memory cells that respond more quickly and efficiently to cognate Ag than Tn cells (Williams and Bevan, 2007).

CD8+ T cells can be "programmed" by short-term access to Ag-presenting DCs to allow differentiation of Teff and memory cells, indicating that CD8+ Tn cells can make early fate decisions (Williams and Bevan, 2007). However, although specific T cell markers have been correlated with memory differentiation (Joshi et al., 2007; Kaech et al., 2002; Sarkar et al., 2008; Wherry et al., 2007), most of these markers appear only on day 4 or later after Ag encounter. To date, reliable standardized in vivo models that can be "tuned" to either induce or fail to induce T cell memory have been missing.

Here, we used multiphoton intravital microcopy (MP-IVM) in mouse popliteal LNs (popLNs) to analyze how and when interactions between $CD8^+$ Tn cells and Ag-presenting DCs influence effector and memory differentiation. This study was informed by earlier findings that $CD8^+$ T cells are primed in LNs in three phases (Mempel et al., 2004). Phase 1 can last up to ~8 hr and is characterized by transient T cell interactions with Ag-pulsed DCs. T cells integrate the antigenic stimuli from each encounter until the cumulative signal triggers phase 2 when T cells form a long-lasting contact with a single DC (Mempel et al., 2004). The higher the concentration of cognate pMHCs per DC, the faster T cells reach phase 2 and the shorter is phase 1 (Henrickson et al., 2008). Phase 2 lasts ~12 hr and is accompanied by upregulation of activation markers and cytokine production. Phase 3 begins ~1 day after T cell entry into the LN when T cells return to short interactions and proliferate vigorously. Sequential phases of transient and stable DC-T cell contacts have been independently observed in many systems (Hugues et al., 2004; Mempel et al., 2004; Miller et al., 2004b; Skokos et al., 2007; Stoll et al., 2002); however, it has been unclear whether the stable contacts that define phase 2 are necessary for full-fledged T cell activation, as is widely assumed, or if they simply correlate with T cell differentiation to Teff and memory cells. It has also been uncertain whether and how early interaction dynamics influence Tn cell fate, particularly the acquisition of longevity and self-renewal capacity needed for immunologic memory.

To address this question, we adapted an experimental strategy whereby Ag-specific $CD8^+$ Tn cells are allowed to encounter in LNs a finite number of DCs that were pulsed with either a low or a high dose of a naturally occurring viral peptide Ag (Henrickson et al., 2008). This enabled us to ask how T cells make fate decisions in vivo while Ag dose and persistence were precisely controlled. Our approach may not mimic a typical infection where the kinetics of Ag availability are more complex; however, similar conditions might be encountered when T cells respond to nonreplicating vaccine Ags. We found that only DCs pulsed with the high Ag dose supported phase 2-like tight interactions with cognate T cells, but DCs pulsed with either Ag dose induced T cell proliferation and Teff cell differentiation. The differential interactive behavior induced by high- versus low-dose Ag-pulsed DCs was paralleled by distinct transcriptional programs in activated T cells. Moreover, only T cells that interacted with DCs presenting high-dose Ag gave rise to sustained immunological memory, suggesting that information exchange in phase 2 is critical for long-term protection and avoiding immunological amnesia.

RESULTS

MP-IVM Studies of Low-Dose Peptide-Pulsed DCs Interacting with Ag-Specific T Cells

To control the dose and availability of Ag in mouse LNs, we used a protocol that delivers Ag by footpad injection of peptide-pulsed DCs, so Ag availability was limited to a few hundred DCs that migrated to the draining popLN. Tn cells were injected intravenously (i.v.) 18 hr later, allowing a few thousand transferred cells to access the popLN before further entry was blocked (Henrickson et al., 2008; Mempel et al., 2004). This protocol ensures that all measured responses were due to locally confined T cell-APC interactions (Figure 1A).

For Ag pulsing, splenic DCs were incubated in vitro for 1 hr with varied doses of $gp_{33–41}$ (KAVYNFAT**C**, "C-peptide"), an immunodominant peptide of lymphocytic choriomeningitis virus (LCMV) that complexes with MHC H-$2D^b$ and activates $CD8^+$ Tn cells from TCR transgenic P14 mice (Pircher et al., 1989). During DC pulsing, endogenous peptides in surface-expressed H-$2D^b$ are replaced by C-peptide; the fraction of C-peptide loaded H2-D^b complexes on DCs depends on the peptide concentration in the pulsing buffer and decreases over time as noncovalently bound C-peptide dissociates (Henrickson et al., 2008).

Pulsing conditions were chosen after measuring the ability of DCs pulsed with different C-peptide concentrations to yield Tn cell proliferation in vivo. A pulsing concentration of 1 μM was the lowest at which pulsed DCs reproducibly induced proliferation of >95% of P14 cells (Figure 1B). MP-IVM was performed with DCs pulsed with either the threshold dose (1 μM) of C-peptide (1C DC) or with a higher dose, 100 μM (100C DC), which provided maximal initial loading of DC-expressed H2-D^b. Pulsed DCs were washed, labeled fluorescently, and injected into a footpad. Eighteen hours later, fluorescent P14 Tn cells and differentially labeled control OT-I Tn cells (bearing an irrelevant TCR) were coinjected i.v.; after 2 hr, further T cell homing to LNs was blocked with anti-L-selectin to synchronize intranodal T cell dwell-time and permit exact kinetic studies of T cell activation (Figure 1A). At different times thereafter, mice were anesthetized and the popLN draining the injected footpad was prepared for MP-IVM.

Earlier studies show that P14 Tn cells that encounter DCs pulsed with an intermediate dose (10 μM; 10C) of C-peptide engage in three interactive phases (Mempel et al., 2004). Also, work with an altered peptide ligand for P14 T cells, KAVYNFAT**M** (M-peptide), which has a higher affinity and longer half-life in H2-D^b than C-peptide (Achour et al., 2002; Boulter et al., 2007; Henrickson et al., 2008), shows that M-peptide concentration is reciprocally correlated with the duration of the first phase during which T cells undergo brief serial contacts with DCs (Henrickson et al., 2008). T cells that encounter DCs bearing a higher amount of M-peptide require fewer interactions to initiate phase 2, which is defined as the period during which the median T cell-DC contact duration is ≥30min (Mempel et al., 2004). Any M-peptide dose that supports P14 cell priming also induces phase 2-like contacts, while phase 2 is absent when DCs are pulsed with a M-peptide dose just below the activation threshold (Henrickson et al., 2008). This correlation of interactive behavior and proliferative response seems consistent with the idea that phase 2-like DC-T cell conjugates are a prerequisite for T cell activation (Fooksman et al., 2009).

P14 T cell interactions differed when exposed to 1C DCs (Figures 1C–1H), which failed to promote phase 2 interactions (Table 1; see Movies S1–S5 available online). At most, ~3.8% of contacts lasted ≥30min at any time from 5 to 10 hr after T cell transfer when phase 2 is usually observed (Henrickson et al., 2008; Mempel et al., 2004). In contrast, phase 2-like tight conjugates were prevalent when 100C DCs or 10 μM M-peptide pulsed DCs (10M DCs) were used (Figures 1D–1F; Movie S6). Of note, although the mean contact duration of P14 cells with 1C DCs never exceeded ~7 min, these cognate interactions were still subtly but significantly prolonged when compared to

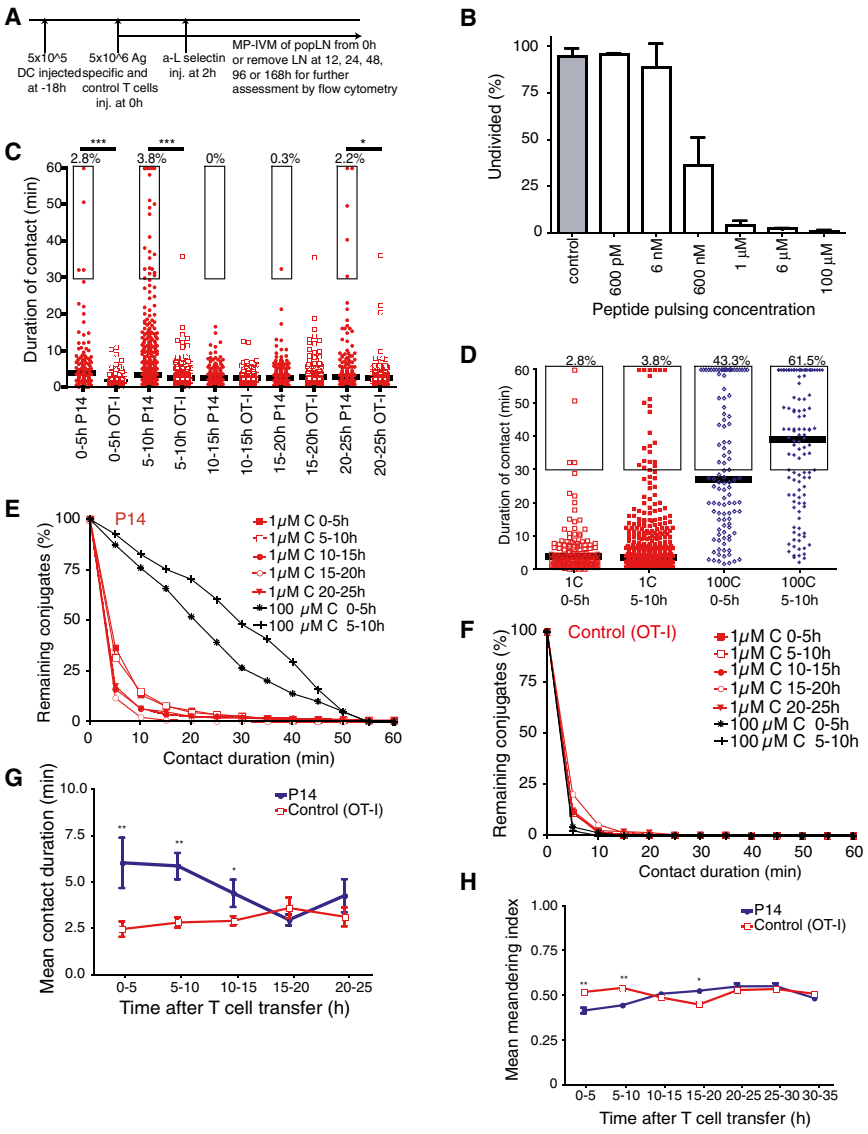

Figure 1. P14 T Cells Maintain Brief Interactions with 1 μM C-Peptide Pulsed DCs

(A) Experimental paradigm for study of P14 *Tcra*$^{-/-}$ (P14) and control (OT-I Rag1$^{-/-}$) T cell interactions with peptide-pulsed DCs. Unless otherwise mentioned, this will be the protocol for experiments throughout the paper.

(B) Percentage of antigen-specific (P14) T cells at 48 hr that remain unproliferated after exposure in vivo to DCs pulsed with various concentrations of C-peptide (error bars are mean ± SD).

(C–G) P14 and control stated above (that OT-I are *Rag1*$^{-/-}$) T cell interactions with DCs pulsed with 1 μM or 100 μM C-peptide pulsed DCs (1C or 100C, respectively) were visualized in popLNs by MP-IVM at the indicated time points after T cell injection i.v. (C) Duration of P14 T cell-1C-peptide-pulsed DC (1C DC) contacts at various time points after T cell transfer was assessed in 3D reconstructed videos (error bar at median, *** = $p < 0.0001$, ** = $p = 0.0013$ by Mann-Whitney). (D) Duration of T cell-DC contacts with 1C DC or 100C DC at various time points after T cell transfer was assessed in 3D reconstructed videos. P14 and control T cell interactions with 1C versus 100C DCs were visualized in popliteal LNs by MP-IVM from 0–10 hr after T cell injection (bar at median, box surrounds durations of 30–60 min, percentage of events above box). (E and F) Cumulative distribution plots of interaction durations for P14 (E) and control (F) T cells interacting with 1C or 100C. (G) The bootstrap corrected means of the interaction durations between P14 T cells (blue) control T cells (red) with DCs. (1C: n = 2–4 experiments per time point; mean ± 95% confidence interval [CI], ** = $p < 0.0004$ and $p = 0.0008$).

(H) The bootstrap corrected means of the meandering indices (MI) of P14 and control T cells when interacting with 1C or 100C DCs. Cell centroids in 3D were measured by semiautomated cell tracking and the MI was calculated by dividing the displacement for each cell track by the total path length for that cell track. (n = 2–4 expt per timept; mean ± 95% CI, ** = $p < 4 \times 10^{-4}$, * = $p = 0.017$). See also Movies S1–S6.

noncognate interactions of control OT-I cells with either Mann-Whitney test (Figure 1C) or bootstrap corrected mean (Figure 1G).

We also measured the meandering index (MI), the ratio of a migrating cell's linear displacement to the total path length (Henrickson et al., 2008), by using automated custom-designed cell tracking software, which avoids potential observer bias. Free-moving Tn cells in Ag-free LNs have a median MI of ~0.5, whereas phase 2-like DC-T cell interactions confine T cells and reduce the MI to <0.3 (Henrickson et al., 2008)). The median MI of P14 cells encountering 1C DCs during the first 10 hr after T cell transfer was slightly lower than that of control OT-I cells, but always remained >0.4 (Figure 1H). Thus, 1C DCs subtly confined P14 Tn cells, but did not support phase 2-like interactions (Figures 1B–1F).

Proliferation after Tn Cell Exposure to High Versus Low Ag Constellations

Next, we examined the kinetics and magnitude of P14 cell proliferation. CFSE-labeled P14 Tn cells (CD45.2$^+$) were injected i.v. into congenic recipients (CD45.1$^+$) 18 hr after footpad injection of DCs, and CFSE dilution of transferred P14 T cells was monitored (Figure 2A). Consistent with our dose-finding experiments (Figure 1B), both 1C DC and 100C DC induced rapid P14 cell proliferation with nearly identical kinetics during the first 48 hr (Figure 2B), suggesting that CD8$^+$ Tn cells can be activated in vivo without sustained contacts with Ag presenting DCs. However, a strong inflammatory challenge usually induces temporary trapping of T cells in LNs (Shiow et al., 2006). Conceivably, the weak stimulus from 1C DCs might not have exerted this effect, so unstimulated P14 cells could have exited the LN. Thus, it remained theoretically possible that the proliferated cells did not arise from precursors that engaged in transient interactions and instead were progeny of the small fraction (<4%) that underwent stable contacts with 1C DC (Figure 1C).

To account for potential premature exit of undivided Tn cells from LNs, we injected mice at 2 hr after T cell transfer with anti-L-selectin (to block further homing) and FTY-720, a sphingosine-1-phosphate (S1P) receptor agonist that prevents T cell

Table 1. Quantification of T Cell-DC Contact Durations

Time after T Cell Transfer, T Cell Specificity, and DC Peptide Pulsing Dose	Number of Interactions Assessed	Number of Interactions ≥30 min Duration	Percentage of Total
0–5 hr P14, 1C	142	4	2.8
0–5 hr control, 1C	93	0	0
5–10 hr P14, 1C	613	23	3.8
5–10 hr control, 1C	405	1	0.25
10–15 hr P14, 1C	301	0	0
10–15 hr control, 1C	210	0	0
15–20 hr P14, 1C	355	1	0.28
15–20 hr control, 1C	187	1	0.53
20–25 hr P14, 1C	233	5	2.2
20–25 hr control, 1C	230	1	0.43
0–5 hr P14, 100C	104	45	43.3
0–5 hr control, 100C	62	0	0
5–10 hr P14, 100C	109	67	61.5
5–10 hr control, 100C	55	0	0

Summary of the duration of interactions of P14 and control $CD8^+$ T cells with both 100C DCs and 1C DCs from MP-IVM studies in popLN of recipient B6 mice from 0–25 hr after T cell transfer. For each 5 hr bin, the number of total DC-T cell interactions, the number of interactions with a duration of greater than 30 min, the definition of a stable DC-T cell contact, and the percentage of interactions greater than 30 min are shown.

egress from LNs (Mandala et al., 2002). By simultaneously blocking T cell entry and exit, we could accurately monitor the entire LN-resident P14 T cell population regardless of Ag constellation. Thus, we quantified the number of transferred $CFSE^{bright}$ P14 cells that had not proliferated in LNs containing 1C, 100C, or control peptide pulsed DCs (Figure 2C).

Four hours after T cell transfer, similar numbers of undivided P14 cells were recovered from popLNs in all conditions, indicating that early T cell recruitment and retention were not substantially affected by our experimental manipulations (Figure 2C). On days 2 and 4, nearly all P14 T cells in both FTY-720 treated and control recipients of 1C or 100C DCs had divided at least once, whereas Ag-free LNs contained mostly undivided cells (Figure 2C). Thus, essentially all P14 cells that encountered 1C DCs proliferated even though their interactions with DCs were almost exclusively brief and dynamic.

Ag Dose Effects on Effector Burst Kinetics and Tn Cell Apoptosis

Although our proliferation studies provided proof for efficient T cell stimulation by both 1C and 100C DCs, cell division alone might not necessarily predict the ensuing effector burst. Indeed, during the first 48 hr, the absolute number of P14 T cells that had divided at least once was similar in LNs draining 1C DCs and 100C DCs (Figure 3A); however, by 96 hr, LNs that received 100C DCs contained substantially more P14 cells than those that received 1C DCs ($p < 0.03$). When expressed as a percentage of LN-resident lymphocytes (Figure 3B), the frequency of P14 Teff cells at 48 hr was twice as high after treatment with 1C DCs (mean ± SEM: 1.94% ± 0.3%) than with 100C DCs (0.96% ± 0.16%). Although this difference did not reach statistical significance ($p = 0.08$), the degree of CFSE dilution at 48 hr was similar in P14 cells that had encountered 1C and 100C DCs, indicating that the early proliferative advantage in the 1C setting was not due to accelerated division (Figure 2A).

The apparent delay in P14 Teff burst induced by 100C DCs was caused by Ag-induced T cell apoptosis preceding the onset of proliferation; approximately half of the P14 cells exposed to 100C DCs were apoptotic at 24 hr, whereas much less apoptosis was seen with 1C DCs (Figures 3C and 3D). This curtailing of the Teff response by high-dose Ag likely accounted for the lower P14 cell frequency among LN T cells at 48 hr; however, the 100C stimulated cells continued to expand until 96 hr, whereas the P14 cells exposed to 1C DC peaked at 48 hr and then declined (Figure 3B). When 1C DC recipients were treated with FTY-720, the number of P14 cells continued to climb in LNs until day 4 (Figures 3E and 3F), indicating that 1C and 100C DC induced differential egress from LNs after day 2.

CD8+ Teff Function after Low- and High-Dose Ag Exposure

Having determined that 1C and 100C DCs induced equivalent early P14 cell proliferation, we asked whether Ag dose affects effector function by exposing P14 T cells to C-peptide, M-peptide, or control peptide pulsed DCs in popLNs. P14 cells were harvested 20 hr or 48 hr later and restimulated ex vivo to assess effector activity. There was no significant difference in the frequency or magnitude of IFN-γ production in response to 1C or 100C DCs (Figures 4A and 4B). Likewise, when P14 T cells were activated by either 1C or 100C DC for 48 hr, Ag-specific in vivo cytotoxicity was similar (Figures 4C and 4D). Thus, minimal antigenic constellations that do not promote stable contacts with Ag-pulsed DCs can be sufficient to initiate Tn cell activation and Teff differentiation.

Memory Differentiation Correlates with Ag Dose and Stability of T Cell-DC Contacts

How does differential Ag presentation impact T cell memory differentiation? We first tried to address this question by transferring $CD8^+$ T cells from $CD45.2^+$ P14x$Tcra^{-/-}$ donors (from Taconic) into congenic $CD45.1^+$ recipients (from Jackson Labs or Taconic) to monitor long-term persistence and recall of $CD45.2^+$ cells. However, the transferred cells disappeared within ~3–4 weeks (data not shown), suggesting that differences between the P14x$Tcra^{-/-}$ and both $CD45.1^+$ strains (per their vendors on a C57BL/6 background) elicited a host response against cryptic alloantigens (Bhattacharya et al., 2006). Thus, we sought alternatives for tracking of noncongenic transferred T cells while avoiding concomitant activation of endogenous T cells recognizing C-peptide. Because the half-life of C-peptide in $H\text{-}2D^b$ is ~2.4 hr (Henrickson et al., 2008), encounters occurring before 18 hr after DC injection (when P14 Tn cells are transferred) would expose endogenous T cells to higher Ag doses that presumably support stable contacts. P14 cell transfers were deliberately timed so that the cells accessed LNs only when the Ag dose on 1C DCs had fallen below the threshold at which stable contacts occur.

By using two distinct recipient strains that could neither mount an endogenous response against $gp_{33–41}$ nor reject transferred

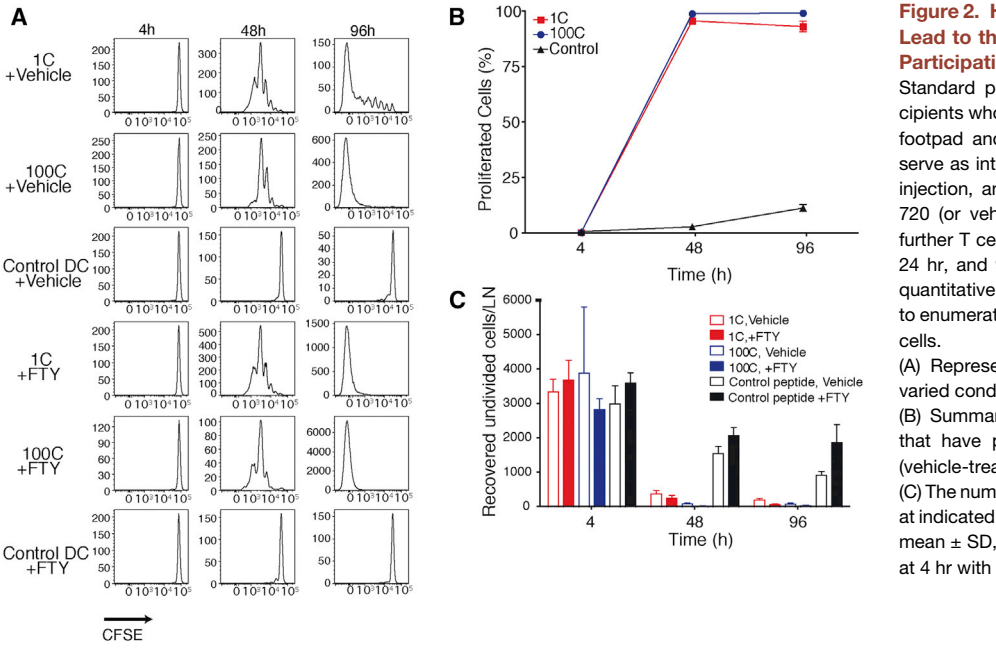

Figure 2. High- and Low-Dose Antigen Both Lead to the Majority of Transferred T Cells Participating in Effector Response

Standard protocol (Figure 1A), with CD45.1 recipients who received 1C or 100C DCs in the right footpad and control DCs in the left footpad (to serve as internal controls). Two hours after T cell injection, anti-L-selectin antibody (Ab) and FTY-720 (or vehicle alone) were injected to prevent further T cell entry and exit, respectively. At 4 hr, 24 hr, and 96 hr, recipients were sacrificed and quantitative flow cytometry with beads was used to enumerate the number of remaining transferred cells.

(A) Representative flow cytometry plots across varied conditions, as labeled.

(B) Summary of percentage of transferred cells that have proliferated at indicated time points (vehicle-treated recipients).

(C) The number of total undivided, transferred cells at indicated time points and conditions (n = 4 expt, mean ± SD, 3–7 mice per condition, except 100C at 4 hr with 2).

P14x*Tcra*$^{-/-}$ Tn cells, we could assess Ag-specific recall responses mediated exclusively by transferred cells. In both settings, we applied our standard protocol for DC and P14 T cell transfer (Figure 1A, but without anti-L-selectin), challenged with LCMV (10^3 plaque-forming units [pfu] i.v.) after 30+ days and 5 days later restimulated CD8 T cells ex vivo with $gp_{33–41}$ to detect IFN-γ-secreting P14 memory cells.

In the first model, we infused naive C57BL/6 mice with M-peptide, which depletes endogenous CD8$^+$ T cells recognizing the $gp_{33–41}$ epitope, creating a "hole" in the endogenous T cell repertoire (Garza et al., 2000) and rendering mice incapable of responding to $gp_{33–41}$ (Figure S1). After LCMV rechallenge, recipients of 1C DCs or control DCs contained equivalently low numbers of $gp_{33–41}$ reactive T cells, whereas 100C DC sensitized mice had generated abundant P14 memory cells (Figure 5A). As a second strategy, we tested the same protocol by using transgenic recipients (OT-Ix*Rag1*$^{-/-}$) that expressed a single irrelevant TCR and could not respond to C-peptide or alloantigens. Again, recipients of control DCs or 1C DCs contained few $gp_{33–41}$ reactive CD8$^+$ T cells, whereas 100C DC recipients had generated ~5-fold more memory cells (Figure 5B). In both experiments, virus-specific T cell responses were assessed as late as 5 days after LCMV challenge, providing ample time for even small memory populations to "catch up." The fact that there was no statistical difference between 1C DC recipients and control mice that harbored only non-antigen-specific Tn cells suggests that 1C DCs completely failed to induce memory.

Transcription Profiles of T Cells Exposed to High- and Low-Dose Antigenic Constellations

To explore at a molecular level how 1C and 100C DC sensitization induce such distinct outcomes in cell-cell interactions and memory differentiation, we compared transcription profiles of P14 T cells by using DNA microarrays (Haining et al., 2008). P14 cells were activated following our standard protocol (Figure 1A) and sorted from single-cell suspensions of popLNs at 12 or 24 hr after transfer. This timing of T cell harvesting was chosen because previous MP-IVM results had shown that an intermediate Ag dose (10C DC) induces phase 2 interactions that are maximal by ~12 hr and resolve after ~20 hr (Mempel et al., 2004), suggesting that the conditions encountered by CD8$^+$ Tn cells within the first day set the stage for a differential fate decision resulting either in long-term memory or an abortive Teff response.

Activation by either 1C or 100C DCs altered the expression of several 1,000 genes that were significantly up- or downregulated compared to Tn cells. Many genes were similarly regulated in both conditions, but a roughly equal number changed in only one activating setting (Figure 6A). These differentially expressed genes increased slightly in number from 12 to 24 hr (Figure 6A). Among the transcripts that changed uniquely at 24 hr in the 100C setting, 57% were upregulated, whereas most uniquely regulated genes in the 1C setting were downregulated (67%). No genes were reciprocally altered relative to Tn cells; i.e., no genes increased in one activation setting and decreased in the other. Principal components analysis (PCA) showed that P14 cell activation by 1C or 100C DCs resulted in transcriptional profiles that were distinct and divergent between 12 and 24 hr but more similar to each other than to Tn cells (Figure 6B).

A gene-set enrichment analysis (GSEA) (Haining and Wherry, 2010) was performed to compare our results to published gene expression profiles from P14 Teff cells on day 8 (d8) after LCMV infection (Wherry et al., 2007). Compared to Tn cells, the d8 effector gene set was significantly enriched in T cells exposed to 1C DCs ($p < 0.001$, FDR < 0.0001) and 100C DCs ($p < 0.001$, FDR < 0.002) at both at 12 hr and 24 hr after stimulation (Figure 6C), indicating that effector differentiation commences as early as 12 hr after activation.

There were also differences between transcriptional states in the 1C and 100C settings, which were evident when results were presented as a heatmap (Figure 6D) or volcano plot

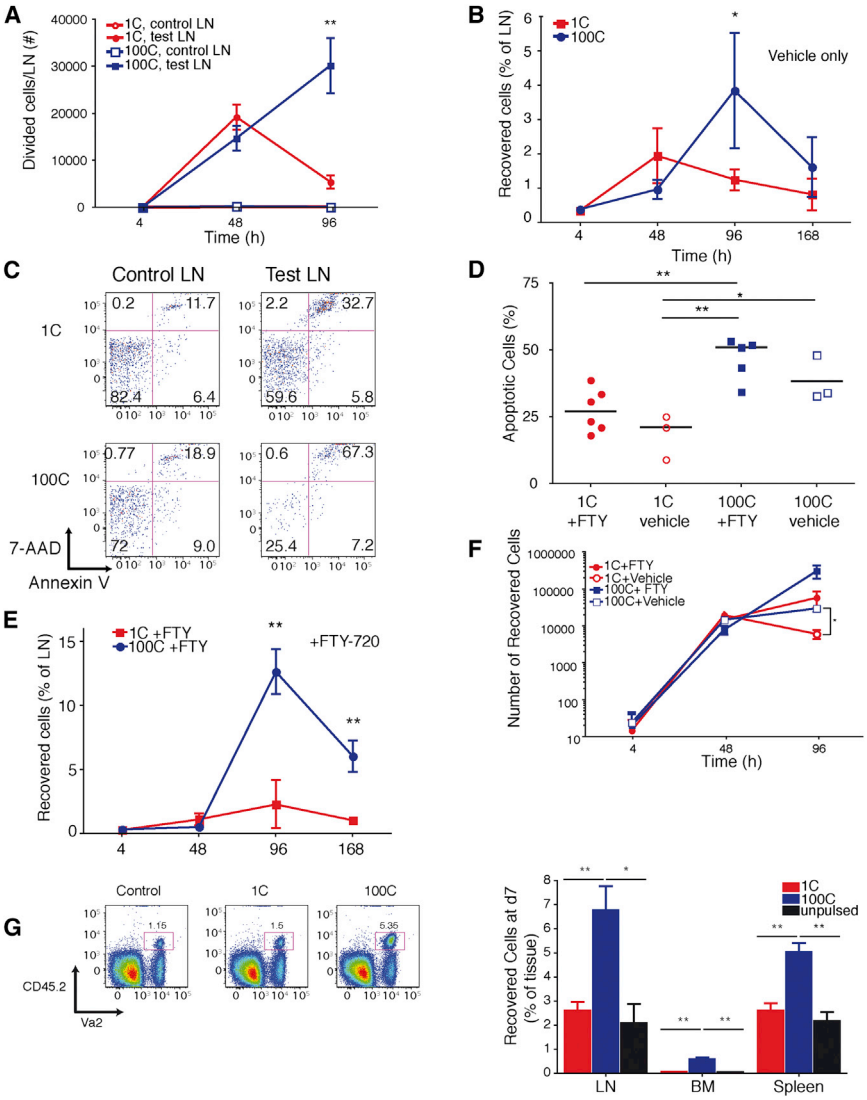

Figure 3. Higher Dose Antigen Eventually Yields Larger Effector Pool after a Larger Early Apoptotic Loss

Standard protocol (Figure 1A), with CD45.1 recipients who received 1C or 100C DCs in the right footpad and control peptide-pulsed DCs in the left footpad (to serve as internal controls). Two hours after T cell injection, anti-L-selectin Ab and FTY-720 (or vehicle alone) were injected to prevent further T cell entry and exit, respectively.

(A, B, E, and F) At 4 hr, 48 hr, 96 hr, or 7 days, recipients were sacrificed and quantitative flow cytometry, with beads, was used to enumerate the number of remaining transferred cells in the popLN. This is presented as (A) the absolute number of recovered CD45.2$^+$ cells recovered at 4 hr, 48 hr, and 96 hr in the LN (vehicle treated; mean ± SEM) and (F) vehicle or FTY treated recipient (mean ± SEM). Number of CD45.2 (transferred and progeny of transferred) cells, as a percentage of total LN cells at each time point, either additionally treated with vehicle (B) or (E) FTY-720 (A and B; E and F: n = 4 expt, 3–7 mice per condition, except 100C at 4 hr with 2; B and E: mean ± SD).

(C and D) Percentage of apoptotic transferred CFSE labeled P14 T cells at 24 hr after T cell transfer (Annexin V+, 7-AAD+), with 1C DC, 100C DC, or DCs pulsed with control peptide, (C) representative flow cytometry, and (D) summary of percentage of cells which are apoptotic at 24 hr (n = 3–6 expt and 3–8 mice per condition, bar at median).

(G) The percentage at d7 of transferred CD4-B220- cells in the LN, CD8$^+$ T cell negative selected spleen, and bone marrow that represents recovered transferred cells. Left shows representative flow cytometry; right shows summary of flow cytometry data (n = 2 expt, four mice per condition).

(Figure 6E). The list of genes differentially expressed between 1C and 100C T cells included several transcriptional regulators, suggesting that day 1 may constitute a cell-fate branch-point for CD8$^+$ T cells (Tables S1A and S1B). We also used GSEA with curated gene sets to assess how gene families involved in specific cellular processes or signaling pathways are modified (Tables S2A and S2B), compared specific molecules of interest, including costimulatory and inhibitory receptors, cytokines and chemokines and their receptors, components of the apoptosis pathway, and genes involved in CD8 T cell exhaustion and effector states (Table S3A), and investigated genes of interest within gene sets identified by GSEA (Tables 3B–SE).

Transcripts for actin and other cytoskeletal genes were upregulated in T cells exposed to 1C DCs (Tables S2A, S2B, and S2D), consistent with the sustained high T cell motility in this condition and formation of serial kinapses with APCs (Moreau et al., 2012). In T cells exposed to 100C DCs, effector cytokines and lineage-specific transcription factors were significantly upregulated compared to the 1C DC setting, including IL-2 (at 24 hr) and IFN-γ (at 12 hr and 24 hr; Tables S1A and S3E). Accordingly, there was a marked enrichment in transcription factors associated with effector and memory differentiation (Cui et al., 2011), including TBX21 (T-bet) and Jun, in 100C DC exposed T cells (Tables S3A and S3C). Given the transcriptional differences in IFN-γ and other cytokines, despite equivalent IFN-γ protein secretion upon in vitro restimulation at 20 hr and 48 hr (Figures 4A and 4B), we examined IFN-γ production at 96 hr (Figure S2). Consistent with the preceding upregulation of IFN-γ messenger RNA, T cells exposed to 100C DCs secreted significantly higher amounts of IFN-γ at 96 hr than T cells that had encountered 1C DCs. 100C DC-exposed T cells also upregulated the Stat3 pathway (Tables S3A and S3C), which is upregulated in memory precursors (Cui et al., 2011; Siegel et al., 2011). This differential pattern of transcription factors and regulatory molecules is consistent with the finding that stimulation with 1C versus 100C DCs profoundly influences the fate of P14 cells. Finally, 100C DC exposed T cells selectively upregulated many coinhibitory molecules (Odorizzi and Wherry, 2012; Pardoll, 2012; Youngblood et al., 2011), including PD-1, CD200, LAG-3, and CTLA-4 (Tables S1A and S2A), which might reflect a mechanism

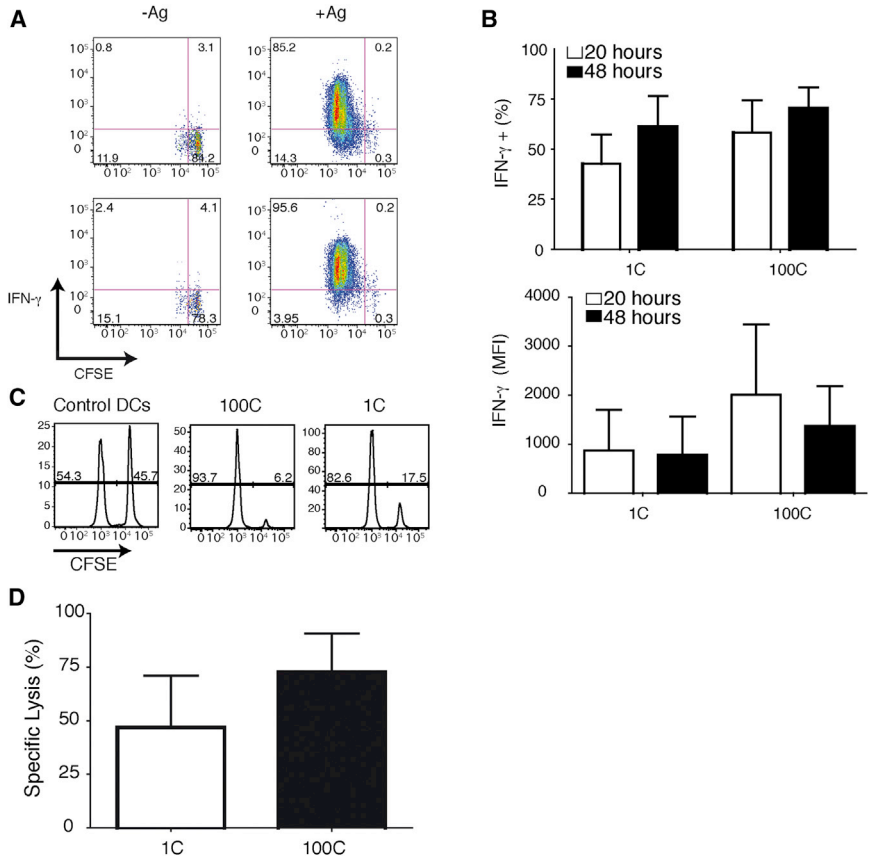

Figure 4. Effector Function Is Equivalent on Whether or Not T Cells Engage in Stable Contacts with DCs

(A and B) Standard protocol (Figure 1A), with CD45.1 recipients who received 1C or 100C DCs in the right footpad and control DCs injected in left footpad to serve as internal controls. At 20 hr and 48 hr, popLN were harvested and IFN-γ production was measured by cell-surface capture. (A) Representative flow cytometry plots at 48 hr. (B) Percentage of IFN-γ positive transferred cells from 1C or 100C at 20 hr and 48 hr after P14 T cell transfer. IFN-γ positivity is calculated based on IFN-γ secretion from P14 T cells exposed to test peptide-pulsed DCs corrected for the amounts of secretion from P14 T cells exposed to control peptide-pulsed DCs. (Percentage of IFN-γ positivity by experiment ± SEM and MFI is presented per mouse, mean ± SD; n = 4 or 5 mice 1C at 20 and 48 hr, n = 3 or 4 mice 100C at 20 and 48 hr; n = 2 expt at 20 hr, n = 3 expt at 48 hr.)

(C and D) Control peptide DC (left), 100C DC (middle), or 1C DC (right) were injected into the footpads of recipient congenic (CD45.1) mice. P14 T cells were injected i.v. 18 hr later. After an additional 48 hr, two target polyclonal B cell populations (one pulsed with 10 μM M-peptide, labeled with 2 μM CFSE; the other non-peptide pulsed, labeled with 0.1 μM CFSE), were mixed at a 1:1 ratio and injected i.v. Six hours later, the ratio of $CFSE^{hi}$:$CFSE^{lo}$ B cells was assessed in the popLN. (C) Representative plots of target cells after in vivo lysis (representative of 3–9 mice per group, n = 2 [100C] or 4 [all other concentrations] expt). (D) Pooled specific lysis of Ag pulsed target cells (per mouse, mean ± SD. n = 3–9 mice per group, n = 2 [100C] or 4 [all other concentrations] expt). Percent specific lysis is calculated as (1 − [ratio of unprimed/ratio primed] × 100), where the ratio is %($CFSE^{lo}$ nonpeptide pulsed)/(%$CFSE^{hi}$ peptide-pulsed) among transferred $CFSE^{+}$ target B cells. See also Figure S2.

to protect activated T cells from activation-induced cell death in an ongoing response.

DISCUSSION

Optimal $CD8^{+}$ T cell responses ensue when mature DCs present Ag at a dose and duration sufficient to result in Tn cell activation and differentiation into short-lived Teff and long-lived self-renewing memory cells. We know little about the signals that determine whether, how, and what kind of memory cells arise, but these decisions are thought to be regulated, in part, by the dynamics of Tn cell interactions with DCs (Hugues, 2010). During the first 48 hr after Tn cell entry into a LN containing DCs pulsed with a high dose of Ag, these interactions usually follow a three-phase program (Mempel et al., 2004). The duration of phase 1, wherein Tn cells undergo short, serial encounters with DCs, is inversely correlated with Ag dose (Henrickson et al., 2008). Phase 2 features prolonged, stable conjugates during which T cells commence cytokine production. Finally, during phase 3, T cells return to short contacts and proliferate rapidly (Henrickson et al., 2008; Mempel et al., 2004).

It has been unclear how the interaction dynamics during each phase influence immunological outcome. An early clue came from in vitro imaging of T cells interacting with DCs in a collagen gel, which showed that T cells proliferate even when they undergo only transient interactions (Gunzer et al., 2000). While engaging in transient contacts in vivo, T cells are thought to integrate stimuli during each APC encounter until the cumulative signal exceeds a threshold for phase 2 transition (Henrickson et al., 2008). The mechanism for in vivo integration of serial activation signals is unknown, but in vitro work has implicated the Ras family of GTPases (Das et al., 2009) and the Akt pathway (Kim et al., 2012). Phase 2 begins when the median duration between Tn cells and DCs exceeds 30 min. This definition was chosen because Tn cells require ~30 min to form a mature immunological synapse, a dynamic structure at the interface with APCs that is stabilized by LFA-1 on T cells binding the adhesion molecule ICAM-1 on APCs (Dustin and Groves, 2012; Lee et al., 2002). LFA-1–ICAM-1 interactions are also needed for stable Ag-driven T cell/DC contacts in LNs, and ICAM-1-deficient DCs presenting a high Ag dose fail to retain Teff cells at d12 after activation (Scholer et al., 2008). Experimental manipulations that induce T cell tolerance rather than Teff responses, e.g., Ag targeting to immature DCs or promotion of coinhibitory signaling in T cells, result in enhanced T cell motility and lack of stable T cell/DC contacts (Fife et al., 2009; Hugues et al., 2004; Schneider et al., 2006). However, for T cell priming by fully mature wild-type DCs, it had been widely assumed that tight interactions with sustained TCR signaling are needed (Fooksman et al., 2009; Iezzi et al., 1998). Indeed, many MP-IVM studies use reduced T cell motility and clustering with DCs as a surrogate parameter for T cell activation.

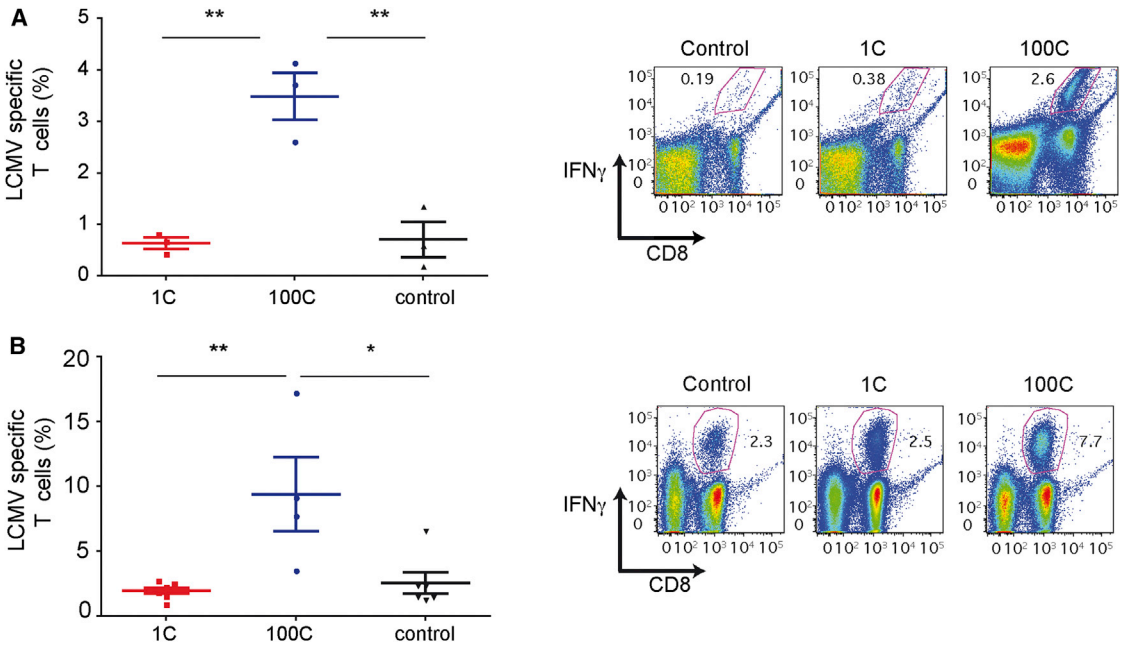

Figure 5. Memory Differentiation Is Impaired without Stable DC-T Cell Contacts

(A and B) Purified CD11c$^+$ DCs were pulsed with 10 μM control-peptide (or no peptide), 1C, or 100C and injected into the right footpad of recipient mice (in A, peptide-depleted C57BL/6 recipients, in B, OT-I recipients) with LPS. 5 × 10^6 P14 T cells were injected i.v. 18 hr later. At d30+ after T cell transfer, each mouse was infected i.v. with 10^3 pfu LCMV Armstrong, the spleens harvested at d5 p.i., and IFN-γ was stained by ICCS after a 5 hr ex vivo stimulation with (+) or without (–) 1 μM C-peptide at 37°. (A) C57BL/6 recipients were treated at d10, 7, and 4 with high-dose M-peptide to deplete them of Ag-specific cells. Upper graph shows a summary of CD8$^+$ IFNγ$^+$, and lower graph shows representative flow cytometry. (n = 3 expt, 3–5 mice, per condition; mean ± SEM). (B) Recipients are OT-I *Rag1*$^{-/-}$. Upper graph shows a CD8$^+$ IFN-γ$^+$ and lower graph shows representative flow cytometry. Of note, in the OT-I recipients there were occasionally animals with extreme splenomegaly and expansion of lymph nodes (in all conditions), which were excluded from analysis in all settings. (n = 3–5 expt, 4–7 mice per condition, mean ± SD per mouse).

Our earlier studies with M-peptide, which has a higher affinity and longer half-life in H2-D^b than C-peptide, seem consistent with this idea (Henrickson et al., 2008). Although pMHC complexes with either C- or M-peptide have similar affinity for the P14 TCR, DCs pulsed with the threshold peptide dose needed to induce P14 proliferation support distinct interaction dynamics; P14 cells that encounter threshold dose M-peptide pulsed DCs transition to phase 2 (Henrickson et al., 2008), but they remained in phase 1 when C-peptide was presented (this study). The most likely explanation for this differential response is the distinct half-life of complexes formed by M- versus C-peptide with H2-D^b (~6 hr versus ~2.4 hr, respectively [Henrickson et al., 2008]). Thus, after P14 cells encounter DCs presenting an amount of Ag that is sufficient to trigger TCR signaling, but insufficient to promote rapid transition to stable contacts, the T cells continue to migrate, accumulating serial activation signals. During this information-gathering period, pMHC complexes disintegrate at a constant rate, which is higher for C- than M-peptide. After several hours, the P14 cells activate LFA-1 enabling sustained contacts, but only with DCs presenting a sufficient amount of Ag to support synapse formation because TCR signaling is needed for LFA-1 to assume a high affinity state and/or to redistribute toward and within the emerging synapse. Long-lived pMHC complexes with M-peptide remain available at this time point, but C-peptide dissipates much faster, so P14 cells cannot find suitable binding partners to engage in phase 2 interactions.

How do the dynamics of T cell–APC interactions affect T cell responses? Clearly, stable contacts are not needed to initiate effector responses by CD8$^+$ T cells in vivo; both 1C and 100C DC induced efficient population-wide proliferation and Teff differentiation of LN-resident Ag-specific Tn cells However, they did so with distinct kinetics and consequences: exposure to high-dose Ag triggered a transient early apoptotic contraction of the responder population (likely due to AICD), followed by vigorous and sustained expansion of LN-resident T cells for ~96 hr and long-term memory formation. By contrast, at the 1C threshold dose, early T cell apoptosis was modest, but after 48 hr the effector pool underwent accelerated attrition, ultimately leading to a complete loss of Ag-experienced cells. While cytokine production and cytotoxicity were equivalent for T cells exposed to 1C and 100C DCs through 48 hr, proliferation and IFN-γ production by 1C T cells were markedly lower at 96 hr, thus reflecting at a protein level the transcriptional differences that appeared as early as 24 hr after Ag encounter.

We used two approaches to study memory differentiation, which each allowed transfer of P14 Tn cells into recipients that lacked gp$_{33–41}$ responsive T cells, so the transferred cells could be identified later based on their Ag responsiveness. Both models restricted a short-lived nonproliferating Ag to a small number of DCs in a single popLN. To ensure that the number of P14 cells that encountered Ag was sufficient for detection and analysis, we transferred 5 million P14 Tn cells of which <0.1% were activated before the Ag disappeared.

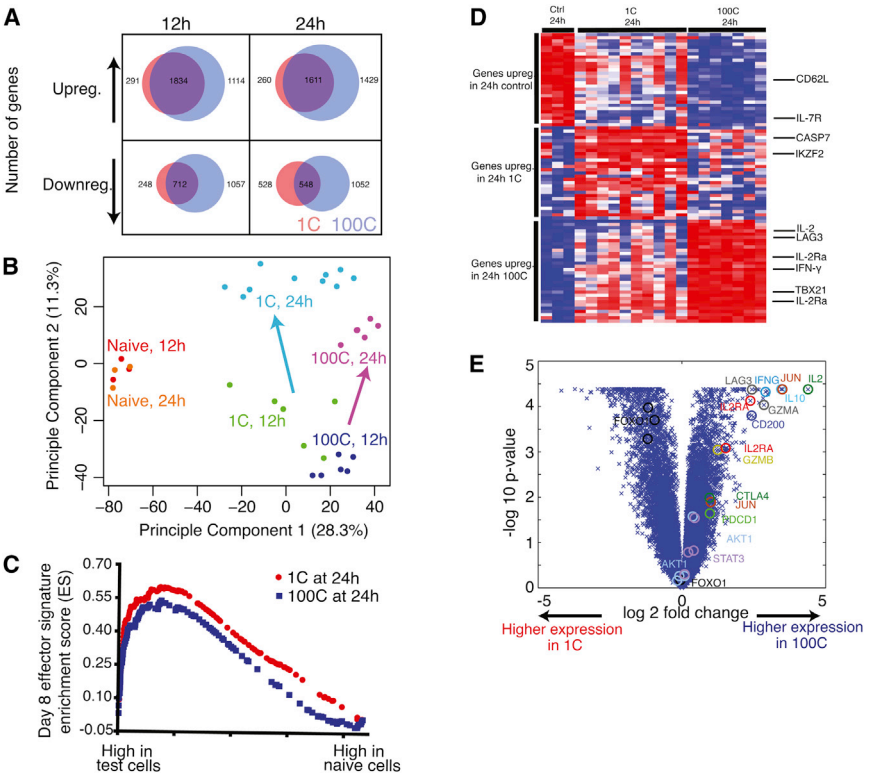

Figure 6. Comparison of cDNA Profiles by DNA Microarray at 12 and 24 hr

Standard protocol (Figure 1A), with two types of recipients who received 1C or 100C or no DCs in the right footpad. The right popliteal LN was harvested at 12 or 24 hr after T cell transfer, single cell suspension created, and stained with CD4, B220, and CD19 (dump channel). Cells were then sorted on a FACSAria as nondoublets, CMFDA$^+$, and dump channel negative. RNA was extracted with standard phenol-chloroform techniques and then concentrated and cleaned with the Agencourt RNAdvance tissue kit. Of the total RNA extracted, an aliquot was then amplified with commercially available kits (NuGEN Pico). Following RNA amplification, aliquots of cDNA from each sample were assayed with the Agilent 2100 bioanalyzer to ensure high-quality amplification prior to fragmentation, labeling, and hybridization to microarray. cDNA was then hybridized on Affymetrix 430_2 arrays for analysis of gene expression patterns at a core facility.

(A) Venn diagrams of differentially expressed genes. Left column shows 12 hr time point; right column shows 24 hr time point. Upper row represents the number of genes that were upregulated for versus naive, and the lower row represents the number of genes that were downregulated versus naive. For each Venn diagram, on the left are genes that are differentially expressed between T cells exposed to 1C versus adoptively transferred naive T cells not exposed to DCs, and on the right are genes differentially expressed between T cells exposed to 100C versus adoptively transferred naive T cells not exposed to DCs. Genes included in these diagrams have fold change statistics >0.5 Wilcoxon p value $\leq$ 0.001.

(B) 2D principal components analysis (PCA) of all six conditions (control, 1C and 100C, each at 12 and 24 hr with each color indicating a separate concentration at a specific time point), with arrows drawn from 12 hr to 24 hr data for each antigenic dose. Principle component (PC) 1 accounts for 28.3% and PC 2 accounts for 11.32%.

(C) Enrichment of the d8 effector signature (Wherry et al., 2007) for the samples from T cells exposed to 1C and 100C samples at 24 hr.

(D) Heatmap of the 30 most differentially expressed genes for each of three sample types (T cells exposed to no DCs, T cells exposed to 1C, and T cells exposed to 100C all at 24 hr) with some genes of interest noted by arrows on the right margin.

(E) Gene expression volcano plot, with –log 10 of the SAM p value on the y axis and log 2 fold change on the x axis, such that genes with higher expression in 1C are on the left and genes with higher expression in 100C are on the right. Genes plotted were expert selected for their known relevance in T cell effector and memory differentiation (arrays: n = 3 for control T cells at 24 hr, n = 10 for 1C at 24 hr, n = 7 for 100C at 24 hr; n = 3 for control T cells at 12 hr; n = 6 for 1C at 12 hr; n = 6 for 100C at 12 hr). See also Figure S1 and Tables S1–S3.

Consequently, unlike in a systemic viral infection, a substantial population of unactivated transferred cells remained in recipients. To measure memory differentiation, we had to distinguish this residual Tn cell population from true memory cells that arose from Ag encounters in the popLN. This was possible because memory cells respond more rapidly than Tn cells to Ag challenge, so memory cells could be revealed by measuring early Ag-induced IFN-γ secretion. No difference was found between recipients of P14 Tn cells that had received 1C DCs or no Ag, but there was a substantial increase in IFN-γ-secreting cells in recipients of 100C DCs, indicating that the latter had developed memory.

These results establish that CD8$^+$ T cells make differential memory fate decisions in vivo as a consequence of the Ag dose presented by DCs. In this context, we must consider three parameters that distinguish how Tn cells experience encounters with 1C versus 100C DCs: (1) the difference in density of cognate pMHC complexes on a DC affects the number of TCRs that are triggered simultaneously (instantaneous signal intensity); (2) the time interval between T cell entry into the LN until cognate pMHC complexes have disappeared from DCs (signal persistence); (3) 100C DCs, unlike 1C DCs, support phase 2-like contacts, so TCR stimulation changes from an intermittent to a continuous mode (signal duration) (Tkach and Altan-Bonnet, 2013). It remains to be determined whether and to what extent each of these parameters contributes to memory differentiation. Moreover, only a small fraction of P14 cells that encountered 100C DCs ultimately entered the memory pool, and it will be important to understand how this subset is selected.

Regardless of the initial C-peptide pulsing dose and mode of interaction, the very short half life of pMHC complexes is expected to result in a 99.9995% loss of C-peptide from pulsed DCs at 24 hr after T cell injection (42 hr after DC pulsing), so P14 cells in the present study did not experience cognate Ag beyond the first day. Thus, signals received by CD8$^+$ Tn cells from DCs within a single day can precipitate a fate choice between a transient effector burst and long-term memory commitment. Accordingly, a recent study with anti-pMHC

antibodies to terminate $CD8^+$ Tn cell access to Ag showed that Ag accessibility must exceed a threshold duration for optimal memory cell differentiation (Blair et al., 2011). Similarly, during microbial infections LN dwell time, proliferation and memory differentiation of $CD8^+$ T cell are inversely correlated with TCR affinity for microbial Ags (Zehn et al., 2009).

It should be noted that the rules of memory-fate commitment are almost certainly more complex when $CD8^+$ T cells respond to infections. Aside from the concomitant stimulation of $CD4^+$ T cells and other leukocytes that influence $CD8^+$ T cells, even pathogen-derived Ags with low affinity for MHC may afford long signal persistence because proliferating pathogens continue to produce antigenic material, and DCs phagocytose and store such material for cross-presentation (Trombetta and Mellman, 2005), whereas the short peptides used here are not cross-presented (Cebrian et al., 2011). Of note, DCs in our system did not present antigenic moieties to stimulate $CD4^+$ T cells, so P14 cells did not receive "help" (Williams and Bevan, 2007); however, we coinjected LPS with DCs to promote in vivo DC maturation. The experimental system described here reflects a reductionist approach allowing quantitative study of early T cell-fate decisions. Our approach delivers a single Ag pulse with a known (short) half-life on mature DCs providing a level of control that is not feasible with an infectious Ag source. In terms of clinical correlate, this model resembles immunization with a subunit vaccine or autologous DC therapy.

Previous work on early $CD8^+$ memory differentiation has traditionally examined Ag-experienced T cells expressing specific markers that predict effector or memory fate (Kaech et al., 2003) and are associated with widespread changes in gene expression (Haining et al., 2008; Kaech et al., 2002; Sarkar et al., 2008; Wherry et al., 2007). There are also transcriptional differences between Teff and memory T cells and between memory T cells and exhausted T cells (Doering et al., 2012), as well as memory precursor T cells in mice (Sarkar et al., 2008) and humans (Chowdhury et al., 2011). However, because well-known memory-fate markers arise only several days after the initial stimulus, the earliest transcriptional signatures of memory precursors were obtained from this late interval, and the time point when activated T cells first reach a memory-fate checkpoint has been unclear, with active research in this area (Best et al., 2013). The present results suggest that this checkpoint is reached in vivo within less than a day of priming.

To begin to address the determinants and consequences of this early checkpoint, we conducted a transcriptome analysis of P14 cells that were sorted from popLNs 12 hr or 24 hr after exposure to 1C or 100C DCs. Our results reveal a dramatic and progressive divergence in transcriptional profiles even though all environmental parameters other than Ag dose were presumably identical. Interestingly, at 24 hr of stimulation, the 100C condition was associated with preferential upregulation of at least three coinhibitory molecules, CTLA-4, LAG-3, and PD-1. Because tight T cell–DC conjugates dissociate around the 24 hr time point (Mempel et al., 2004), it is possible that these molecules are involved in terminating phase 2. Several studies report that coinhibitory signals antagonize the "stop" signal that T cells receive upon TCR engagement (Fife et al., 2009; Schneider et al., 2006). This signal attenuation may also protect T cells from continued Ag stimulation, which might drive T cells toward an apoptosis-prone Teff phenotype (Mitchison, 1964). Thus, phase 2 might be needed to induce a transcriptional program that in aggregate dampens further TCR signaling during the subsequent effector phase and promotes survival and differentiation toward a memory phenotype.

In summary, we describe an experimental strategy in which Ag-specific $CD8^+$ Tn cells encounter in LNs mature DCs that were pulsed with either a low or a high dose of a naturally occurring cognate viral Ag. Only DCs presenting a high Ag dose supported phase 2-like tight interactions, whereas DCs pulsed with either Ag dose induced vigorous early T cell proliferation and Teff differentiation. The differential interactive behavior induced by high- versus low-dose pulsed DCs was paralleled by distinct transcriptional programs in activated T cells, and only T cells that interacted with DCs presenting the high Ag dose gave rise to sustained immunological memory. This suggests that information exchange in phase 2 allows T cells to pass through a critical early checkpoint that fosters Ag-specific long-term protection and avoids immunological amnesia.

EXPERIMENTAL PROCEDURES

Mice

Male C57BL/6 mice (Charles River Laboratories), congenic C57BL/6 ($CD45.1^+$) mice (Taconic Farms or Jackson Laboratories), OT-I $Rag1^{-/-}$, and P14 $Tcra^{-/-}$ mice (Taconic Farms) were used at 6–10 weeks of age. Experiments were performed in accordance with NIH guidelines and approved by the IACUC of Harvard Medical School.

Reagents

M-peptide (KAVYNFATM), C-peptide (KAVYNFATC), and SIINFEKL were purchased from New England Peptides and resuspended in deionized H_20. Anti-L-selectin mAb (Mel-14) was purchased from BD PharMingen or BioExpress. All other mAbs were from BD PharMingen.

Cell Isolation for Adoptive Cell Transfer

DCs were purified by immunomagnetic cell sorting (~98% $CD11c^+$, Miltenyi Biotec) from spleens of C57BL/6 mice that had been implanted with a Flt-3L secreting melanoma, as described (Mora et al., 2003). $CD8^+$ T cells from LNs and spleens of P14 $Tcra^{-/-}$ and OT-I $Rag1^{-/-}$ mice were purified by negative immunomagnetic sorting (Miltenyi Biotec).

Flow Cytometry

Phenotyping of DCs and T cells was performed on a FACSCalibur or FACSCanto analyzer (Becton Dickinson).

LCMV Infections

Mice were infected i.v. with 10^3 pfu LCMV Armstrong at various time points after DC transfer with or without P14 T cell transfer. At d5 after infection, mice were sacrificed and spleens and popLNs removed for flow cytometry of intracellular IFN-γ expression in $CD8^+$ T cells.

Multiphoton Intravital Microscopy

DCs were pulsed with peptide and labeled for 20 min at 37°C with 10 μM 5-(and 6-)-([(4-chloromethyl)benzoyl] amino) tetramethylrhodamine (CMTMR) or 7-amino-4-chloromethylcoumarin (CMAC; Invitrogen). We injected 5×10^5 DCs in 20 μl IMDM (with 10% FCS) containing 10 ng *E. coli* LPS (Sigma) into the right hind footpad of recipient mice. T cell populations were labeled for 15 min at 37°C with 4 μM 5-chloromethylfluorescein diacetate (CMFDA; Invitrogen) or for 25 min at 37°C with 10 μM CMAC (dyes were swapped between experiments). We gave 5×10^6 cells of each subset (1:1 ratio) to recipients i.v. 18 hr after DC injection. After 2 hr, animals received 100 μg Mel-14 i.v. The right popliteal LN was prepared for MP-IVM on a BioRad 2100MP system as described (Mempel et al., 2004).

Statistics

When appropriate, significance of differences was calculated with Mann-Whitney or Student's t test. The bootstrap correction mean was calculated for interaction durations and meandering indices for each data set (n = 100 interactions) (Manly, 1997).

Microarray Data Acquisition

Total RNA was isolated from TriZol with the Agencourt RNAdvance Tissue Kit (Beckman Coulter) and was amplified with the WT-Ovation Pico RNA Amplification and Labeling System (NuGEN). The cDNA was fragmented, labeled, and hybridized to Affymetrix 430_2 microarrays (Affymetrix). The gene expression data set has been submitted to the NCBI/ GenBank GEO database (series entry GSE49274).

ACCESSION NUMBERS

The gene expression data set for the GeneChip Mouse Genome 430 2.0 microarray data has been submitted to the NCBI GenBank GEO database under accession number GSE49274.

SUPPLEMENTAL INFORMATION

Supplemental Information includes two figures, three tables, Supplemental Experimental Procedures, and six movies and can be found with this article online at http://dx.doi.org/10.1016/j.immuni.2013.08.034.

ACKNOWLEDGMENTS

We thank T. Buschman for assistance with programming and G. Cheng and M. Perdue for technical and secretarial assistance, respectively. This work was supported by NIH grants AI069259 and AI072252 to U.H.v.A. and MSTP funding at Harvard Medical School and a Osaka University Immunology Frontier Research Center (iFREC) Postdoctoral Fellowship to S.E.H.

Received: May 19, 2013
Accepted: August 23, 2013
Published: September 19, 2013

REFERENCES

Achour, A., Michaëlsson, J., Harris, R.A., Odeberg, J., Grufman, P., Sandberg, J.K., Levitsky, V., Kärre, K., Sandalova, T., and Schneider, G. (2002). A structural basis for LCMV immune evasion: subversion of H-2D(b) and H-2K(b) presentation of gp33 revealed by comparative crystal structure.Analyses. Immunity *17*, 757–768.

Best, J.A., Blair, D.A., Knell, J., Yang, E., Mayya, V., Doedens, A., Dustin, M.L., and Goldrath, A.W.; Immunological Genome Project Consortium. (2013). Transcriptional insights into the CD8(+) T cell response to infection and memory T cell formation. Nat. Immunol. *14*, 404–412.

Bhattacharya, D., Rossi, D.J., Bryder, D., and Weissman, I.L. (2006). Purified hematopoietic stem cell engraftment of rare niches corrects severe lymphoid deficiencies without host conditioning. J. Exp. Med. *203*, 73–85.

Blair, D.A., Turner, D.L., Bose, T.O., Pham, Q.M., Bouchard, K.R., Williams, K.J., McAleer, J.P., Cauley, L.S., Vella, A.T., and Lefrançois, L. (2011). Duration of antigen availability influences the expansion and memory differentiation of T cells. J. Immunol. *187*, 2310–2321.

Blattman, J.N., Antia, R., Sourdive, D.J., Wang, X., Kaech, S.M., Murali-Krishna, K., Altman, J.D., and Ahmed, R. (2002). Estimating the precursor frequency of naive antigen-specific CD8 T cells. J. Exp. Med. *195*, 657–664.

Boulter, J.M., Schmitz, N., Sewell, A.K., Godkin, A.J., Bachmann, M.F., and Gallimore, A.M. (2007). Potent T cell agonism mediated by a very rapid TCR/pMHC interaction. Eur. J. Immunol. *37*, 798–806.

Casrouge, A., Beaudoing, E., Dalle, S., Pannetier, C., Kanellopoulos, J., and Kourilsky, P. (2000). Size estimate of the alpha beta TCR repertoire of naive mouse splenocytes. J. Immunol. *164*, 5782–5787.

Cebrian, I., Visentin, G., Blanchard, N., Jouve, M., Bobard, A., Moita, C., Enninga, J., Moita, L.F., Amigorena, S., and Savina, A. (2011). Sec22b regulates phagosomal maturation and antigen crosspresentation by dendritic cells. Cell *147*, 1355–1368.

Chowdhury, F.Z., Ramos, H.J., Davis, L.S., Forman, J., and Farrar, J.D. (2011). IL-12 selectively programs effector pathways that are stably expressed in human CD8+ effector memory T cells in vivo. Blood *118*, 3890–3900.

Cui, W., Liu, Y., Weinstein, J.S., Craft, J., and Kaech, S.M. (2011). An interleukin-21-interleukin-10-STAT3 pathway is critical for functional maturation of memory CD8+ T cells. Immunity *35*, 792–805.

Das, J., Ho, M., Zikherman, J., Govern, C., Yang, M., Weiss, A., Chakraborty, A.K., and Roose, J.P. (2009). Digital signaling and hysteresis characterize ras activation in lymphoid cells. Cell *136*, 337–351.

Doering, T.A., Crawford, A., Angelosanto, J.M., Paley, M.A., Ziegler, C.G., and Wherry, E.J. (2012). Network analysis reveals centrally connected genes and pathways involved in CD8+ T cell exhaustion versus memory. Immunity *37*, 1130–1144.

Dustin, M.L., and Groves, J.T. (2012). Receptor signaling clusters in the immune synapse. Annu Rev Biophys *41*, 543–556.

Fife, B.T., Pauken, K.E., Eagar, T.N., Obu, T., Wu, J., Tang, Q., Azuma, M., Krummel, M.F., and Bluestone, J.A. (2009). Interactions between PD-1 and PD-L1 promote tolerance by blocking the TCR-induced stop signal. Nat. Immunol. *10*, 1185–1192.

Fooksman, D.R., Vardhana, S., Vasiliver-Shamis, G., Liese, J., Blair, D., Waite, J., Sacristan, C., Victora, G., Zanin-Zhorov, A., and Dustin, M.L. (2009). Functional Anatomy of T Cell Activation and Synapse Formation. Annu. Rev. Immunol. *28*, 79–105.

Garza, K.M., Chan, S.M., Suri, R., Nguyen, L.T., Odermatt, B., Schoenberger, S.P., and Ohashi, P.S. (2000). Role of antigen-presenting cells in mediating tolerance and autoimmunity. J. Exp. Med. *191*, 2021–2027.

Germain, R.N., and Stefanová, I. (1999). The dynamics of T cell receptor signaling: complex orchestration and the key roles of tempo and cooperation. Annu. Rev. Immunol. *17*, 467–522.

Gunzer, M., Schäfer, A., Borgmann, S., Grabbe, S., Zänker, K.S., Bröcker, E.B., Kämpgen, E., and Friedl, P. (2000). Antigen presentation in extracellular matrix: interactions of T cells with dendritic cells are dynamic, short lived, and sequential. Immunity *13*, 323–332.

Haining, W.N., and Wherry, E.J. (2010). Integrating genomic signatures for immunologic discovery. Immunity *32*, 152–161.

Haining, W.N., Ebert, B.L., Subrmanian, A., Wherry, E.J., Eichbaum, Q., Evans, J.W., Mak, R., Rivoli, S., Pretz, J., Angelosanto, J., et al. (2008). Identification of an evolutionarily conserved transcriptional signature of CD8 memory differentiation that is shared by T and B cells. J. Immunol. *181*, 1859–1868.

Henrickson, S.E., and von Andrian, U.H. (2007). Single-cell dynamics of T-cell priming. Curr. Opin. Immunol. *19*, 249–258.

Henrickson, S.E., Mempel, T.R., Mazo, I.B., Liu, B., Artyomov, M.N., Zheng, H., Peixoto, A., Flynn, M.P., Senman, B., Junt, T., et al. (2008). T cell sensing of antigen dose governs interactive behavior with dendritic cells and sets a threshold for T cell activation. Nat. Immunol. *9*, 282–291.

Hugues, S. (2010). Dynamics of dendritic cell-T cell interactions: a role in T cell outcome. Semin. Immunopathol. *32*, 227–238.

Hugues, S., Fetler, L., Bonifaz, L., Helft, J., Amblard, F., and Amigorena, S. (2004). Distinct T cell dynamics in lymph nodes during the induction of tolerance and immunity. Nat. Immunol. *5*, 1235–1242.

Iezzi, G., Karjalainen, K., and Lanzavecchia, A. (1998). The duration of antigenic stimulation determines the fate of naive and effector T cells. Immunity *8*, 89–95.

Joshi, N.S., Cui, W., Chandele, A., Lee, H.K., Urso, D.R., Hagman, J., Gapin, L., and Kaech, S.M. (2007). Inflammation directs memory precursor and short-lived effector CD8(+) T cell fates via the graded expression of T-bet transcription factor. Immunity *27*, 281–295.

Kaech, S.M., Hemby, S., Kersh, E., and Ahmed, R. (2002). Molecular and functional profiling of memory CD8 T cell differentiation. Cell *111*, 837–851.

Kaech, S.M., Tan, J.T., Wherry, E.J., Konieczny, B.T., Surh, C.D., and Ahmed, R. (2003). Selective expression of the interleukin 7 receptor identifies effector CD8 T cells that give rise to long-lived memory cells. Nat. Immunol. *4*, 1191–1198.

Kim, E.H., Sullivan, J.A., Plisch, E.H., Tejera, M.M., Jatzek, A., Choi, K.Y., and Suresh, M. (2012). Signal integration by Akt regulates CD8 T cell effector and memory differentiation. J. Immunol. *188*, 4305–4314.

Lanzavecchia, A., and Sallusto, F. (2000). From synapses to immunological memory: the role of sustained T cell stimulation. Curr. Opin. Immunol. *12*, 92–98.

Lee, K.H., Holdorf, A.D., Dustin, M.L., Chan, A.C., Allen, P.M., and Shaw, A.S. (2002). T cell receptor signaling precedes immunological synapse formation. Science *295*, 1539–1542.

Mandala, S., Hajdu, R., Bergstrom, J., Quackenbush, E., Xie, J., Milligan, J., Thornton, R., Shei, G.J., Card, D., Keohane, C., et al. (2002). Alteration of lymphocyte trafficking by sphingosine-1-phosphate receptor agonists. Science *296*, 346–349.

Manly, B.F.J. (1997). Randomization, Bootstrap and Monte Carlo Methods in Biology, 2nd Ed. (FL: Boca Raton).

Mempel, T.R., Henrickson, S.E., and Von Andrian, U.H. (2004). T-cell priming by dendritic cells in lymph nodes occurs in three distinct phases. Nature *427*, 154–159.

Miller, M.J., Hejazi, A.S., Wei, S.H., Cahalan, M.D., and Parker, I. (2004a). T cell repertoire scanning is promoted by dynamic dendritic cell behavior and random T cell motility in the lymph node. Proc. Natl. Acad. Sci. USA *101*, 998–1003.

Miller, M.J., Safrina, O., Parker, I., and Cahalan, M.D. (2004b). Imaging the single cell dynamics of CD4+ T cell activation by dendritic cells in lymph nodes. J. Exp. Med. *200*, 847–856.

Mitchison, N.A. (1964). Induction of Immunological Paralysis in Two Zones of Dosage. Proc. R. Soc. Lond. B Biol. Sci. *161*, 275–292.

Mora, J.R., Bono, M.R., Manjunath, N., Weninger, W., Cavanagh, L.L., Rosemblatt, M., and Von Andrian, U.H. (2003). Selective imprinting of gut-homing T cells by Peyer's patch dendritic cells. Nature *424*, 88–93.

Moreau, H.D., Lemaître, F., Terriac, E., Azar, G., Piel, M., Lennon-Dumenil, A.M., and Bousso, P. (2012). Dynamic in situ cytometry uncovers T cell receptor signaling during immunological synapses and kinapses in vivo. Immunity *37*, 351–363.

Odorizzi, P.M., and Wherry, E.J. (2012). Inhibitory receptors on lymphocytes: insights from infections. J. Immunol. *188*, 2957–2965.

Pardoll, D.M. (2012). The blockade of immune checkpoints in cancer immunotherapy. Nat. Rev. Cancer *12*, 252–264.

Pircher, H., Bürki, K., Lang, R., Hengartner, H., and Zinkernagel, R.M. (1989). Tolerance induction in double specific T-cell receptor transgenic mice varies with antigen. Nature *342*, 559–561.

Sarkar, S., Kalia, V., Haining, W.N., Konieczny, B.T., Subramaniam, S., and Ahmed, R. (2008). Functional and genomic profiling of effector CD8 T cell subsets with distinct memory fates. J. Exp. Med. *205*, 625–640.

Schneider, H., Downey, J., Smith, A., Zinselmeyer, B.H., Rush, C., Brewer, J.M., Wei, B., Hogg, N., Garside, P., and Rudd, C.E. (2006). Reversal of the TCR stop signal by CTLA-4. Science *313*, 1972–1975.

Scholer, A., Hugues, S., Boissonnas, A., Fetler, L., and Amigorena, S. (2008). Intercellular adhesion molecule-1-dependent stable interactions between T cells and dendritic cells determine CD8+ T cell memory. Immunity *28*, 258–270.

Shiow, L.R., Rosen, D.B., Brdicková, N., Xu, Y., An, J., Lanier, L.L., Cyster, J.G., and Matloubian, M. (2006). CD69 acts downstream of interferon-alpha/beta to inhibit S1P1 and lymphocyte egress from lymphoid organs. Nature *440*, 540–544.

Siegel, A.M., Heimall, J., Freeman, A.F., Hsu, A.P., Brittain, E., Brenchley, J.M., Douek, D.C., Fahle, G.H., Cohen, J.I., Holland, S.M., and Milner, J.D. (2011). A critical role for STAT3 transcription factor signaling in the development and maintenance of human T cell memory. Immunity *35*, 806–818.

Skokos, D., Shakhar, G., Varma, R., Waite, J.C., Cameron, T.O., Lindquist, R.L., Schwickert, T., Nussenzweig, M.C., and Dustin, M.L. (2007). Peptide-MHC potency governs dynamic interactions between T cells and dendritic cells in lymph nodes. Nat. Immunol. *8*, 835–844.

Stoll, S., Delon, J., Brotz, T.M., and Germain, R.N. (2002). Dynamic imaging of T cell-dendritic cell interactions in lymph nodes. Science *296*, 1873–1876.

Tkach, K., and Altan-Bonnet, G. (2013). T cell responses to antigen: hasty proposals resolved through long engagements. Curr. Opin. Immunol. *25*, 120–125.

Townsend, A., and Bodmer, H. (1989). Antigen recognition by class I-restricted T lymphocytes. Annu. Rev. Immunol. *7*, 601–624.

Trombetta, E.S., and Mellman, I. (2005). Cell biology of antigen processing in vitro and in vivo. Annu. Rev. Immunol. *23*, 975–1028.

von Andrian, U.H., and Mempel, T.R. (2003). Homing and cellular traffic in lymph nodes. Nat. Rev. Immunol. *3*, 867–878.

Wherry, E.J., Ha, S.J., Kaech, S.M., Haining, W.N., Sarkar, S., Kalia, V., Subramaniam, S., Blattman, J.N., Barber, D.L., and Ahmed, R. (2007). Molecular signature of CD8+ T cell exhaustion during chronic viral infection. Immunity *27*, 670–684.

Williams, M.A., and Bevan, M.J. (2007). Effector and memory CTL differentiation. Annu. Rev. Immunol. *25*, 171–192.

Youngblood, B., Oestreich, K.J., Ha, S.J., Duraiswamy, J., Akondy, R.S., West, E.E., Wei, Z., Lu, P., Austin, J.W., Riley, J.L., et al. (2011). Chronic virus infection enforces demethylation of the locus that encodes PD-1 in antigen-specific CD8(+) T cells. Immunity *35*, 400–412.

Zehn, D., Lee, S.Y., and Bevan, M.J. (2009). Complete but curtailed T-cell response to very low-affinity antigen. Nature *458*, 211–214.

Zinkernagel, R.M., and Doherty, P.C. (1974). Immunological surveillance against altered self components by sensitised T lymphocytes in lymphocytic choriomeningitis. Nature *251*, 547–548.